JOURNAL OF Materials CHEMISTRY

Formation of new tungsten bronzes: electrochemical zinc insertion in WO_3

A. Martínez-de la Cruz,*[a]† Leticia M. Torres-Martínez,[a] F. García-Alvarado,[b] E. Morán[c] and M. A. Alario-Franco[c]

[a]*Facultad de Ciencias Químicas, División de Estudios Superiores, Universidad Autónoma de Nuevo León, Apartado Postal 1625, Monterrey, N.L., Mexico*

[b]*Facultad de Ciencias Experimentales y Técnicas, Universidad San Pablo-CEU, Urb. Montepríncipe, Apd. Correos 67, Boadilla del Monte, Madrid, Spain*

[c]*Departamento de Química Inorgánica, Facultad de Ciencias Químicas, Universidad Complutense, 28040 Madrid, Spain*

New tungsten bronzes have been synthesised by electrochemical zinc insertion in monoclinic WO_3. Through 'electrochemical spectroscopy' we have detected that zinc insertion proceeds by a three-step reduction process. X-Ray diffraction shows that these steps are associated with the formation of different single phases of variable composition Zn_xWO_3: monoclinic for $x=0$–0.01, tetragonal for $x=0.05$–0.09 and cubic for $x=0.2$–0.3.

Introduction

Bronzes have been widely studied owing to their interesting chemical, electrical and optical properties.[1] The tungsten bronzes, with general formula M_xWO_3, are the compounds most extensively studied in this family. The common structural feature of these materials is that of WO_6, which is derived from the well known ReO_3 structure, and consists of octahedra with shared corners. These structural arrangements provide empty tunnels, running parallel to the *b*-axis, where ions can be accommodated. Distortions from the major ideal type occur as a function of the inserted ion content. This is the case for monoclinic WO_3 (m-WO_3) where a gradual insertion of M ions parallels the structural transformation taking place when WO_3 is heated. As the concentration of inserted ion increases, distortions from the cubic ideal symmetry (ReO_3) tend to disappear. This happens, for example, when sodium is inserted. The different Na_xWO_3 compositions that are formed are, firstly monoclinic, then orthorhombic, afterwards tetragonal and, finally cubic, as x is increased from 0–0.93.[2]

Although a large variety of bronzes formed using monovalent ions has been studied, bronzes containing divalent ions as for example Zn^{2+} have not been so widely studied. In this work we present a study of the formation of zinc tungsten bronzes. Among the different preparative routes for the synthesis of tungsten bronzes, we have selected electrochemical insertion reactions to carry out the synthesis of Zn_xWO_3. The main advantage in using this technique is that the redox potential, rate of insertion and stoichiometry can all be controlled while discharging the appropriate cell, allowing intermediate phases, Zn_xWO_3, to be prepared. Using 'step potential electrochemical spectroscopy'[3] we have detected both single-phase regions (solid solutions) and two-phase domains formed during the insertion reaction from which we could select the Zn_xWO_3 sample to be obtained and studied by X-ray diffraction. Usually, structural rearrangements associated with guest–host matrix interactions can be studied by X-ray diffraction, which is the case for the Zn_xWO_3 samples studied here.

Experimental

The zinc insertion study was carried out by electrochemical methods in *Swagelok* type cells[4] containing WO_3 (Merck, 99%) as the electroactive material. For the cathode a pellet obtained by pressing 100–150 mg of a mixture containing the active material, carbon black and ethylene–propylene–diene terpolymer (EPDT) as binder, was used. Since the green–yellow m-WO_3 is not a good electronic conductor, a ratio 60 : 39 : 1 of active material : carbon black : EPDT was used. A foil of metallic zinc (Aldrich, 99.999%) was used as the anode. As the electrolyte, a 0.2 mol dm^{-3} solution of $Zn(CF_3SO_3)_2$ in propylene carbonate (PC)–dimethyl sulfoxide (DMSO) (1 : 4) was used.[5] Electrochemical experiments were done in potentiostatic mode using the step potential electrochemical spectroscopy technique (SPECS).[3] In a typical SPECS experiment, the voltage scanning rate was set at ± 10 mV, 6 h between 1.2 and 0.01 V *vs.* Zn^{2+}–Zn^0, the variation of current with time was recorded at each potential level.

The synthesis of bronzes Zn_xWO_3 was also carried out by an electrochemical insertion method. However using this method the cathodes were obtained by pressing a carbon-free mixture (99.5 : 0.5 ratio of WO_3 : EPDT). Cells were discharged up to a certain composition at a scanning voltage rate of -10 mV, 12 h. When the condition $|I|<|I_0|/100$ was satisfied, the step duration was interrupted and the next voltage step was applied.

Structural characterisation was done by X-ray diffraction using a Siemens D-5000 diffractometer with Cu-Kα radiation (1.5418 Å). Samples were run with a step size of 0.05° using W as internal standard. Moisture sensitive samples were protected during diffracted X-ray collection by the use of a tight sealed sample holder with a beryllium foil window, which was always loaded inside a glove box. Resistivity measurements of some samples, of composition Zn_xWO_3, were done using pellets of 0.2 cm^2 area using the well known four-point method.[6]

Results and Discussion

The X-ray diffraction pattern of the commercial oxide mainly corresponded to m-WO_3, the most stable polymorph at room temperature.[7] Since the triclinic to monoclinic transition occurs at 17 °C, we were not surprised that some weak reflections of the triclinic polymorph were also detected. We used the commercial oxide directly as the active material in our electrochemical cells since the intensities of the triclinic reflections were very weak.

†E-mail: azmartin@ccr.dsi.uanl.mx

(*a*) Electrochemical characterisation

Fig. 1 shows the voltage–composition plot obtained from the first charge-discharge cycle of a cell containing m-WO_3 as the active material in the cathode. It can be observed that electrochemical zinc insertion and deinsertion is feasible in m-WO_3. The reaction proceeds through different processes as can be deduced from the evolution of the cell voltage with x in Zn_xWO_3; different regions labelled as I, II, III, *A* and *B* are observed. The regions where a continuous variation of the potential with composition is observed correspond to single-phase regions (I, II and III) whereas the voltage plateaus, *A* and *B*, are assigned to two-phase regions which are bounded by points of inflection at definite changes in slope of the potential–composition curve.

In order to check our first interpretation we analysed the potentiostatic experiment in more detail, observing the current relaxation with time at each voltage step. Fig. 2 shows these data for the discharging curve. For high potential values, between 1.25 and 0.6 V, only small currents are detected and the cell exhibits a low capacity. For low potential values, below 0.6 V, the current increases reaching a maximum value at 0.55 V *vs.* Zn^{2+}–Zn^0. In this region, peak *A* (Zn_xWO_3; $0.01<x<0.05$), the behaviour of current with time is far from a $t^{-1/2}$ law. Hence we deduced that the diffusion of the zinc ions is not the process that rules the insertion reaction. When a different scan rate was used, peak *A* shows a noticeable change of shape, see Fig. 3. This behaviour confirms that the system is crossing a two-phase domain. In this case, the shape of the peak *A* in the *I*–*E* diagram is asymmetrical with a linear slope whose intercept with the zero current is at the open-circuit two-phase equilibrium value.[8] On the basis of the different experiments carried out, this equilibrium value is approximately 0.58 V *vs.* Zn^{2+}–Zn^0. For potentials below 0.38 V, in the *B* peak, the current *vs.* time plot exhibits a clear anomalous behaviour that indicates that the system is again crossing another two-phase domain with an equilibrium value of 0.43 V *vs.* Zn^{2+}–Zn^0. The corresponding compositions of this region are Zn_xWO_3 with $0.09<x<0.2$.

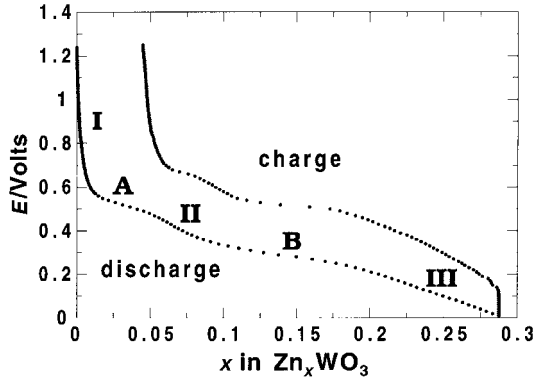

Fig. 1 Voltage–composition plot for a charge–discharge cycle of a cell with configuration Zn||WO_3. The cycling was done under potentiostatic mode (see Experimental).

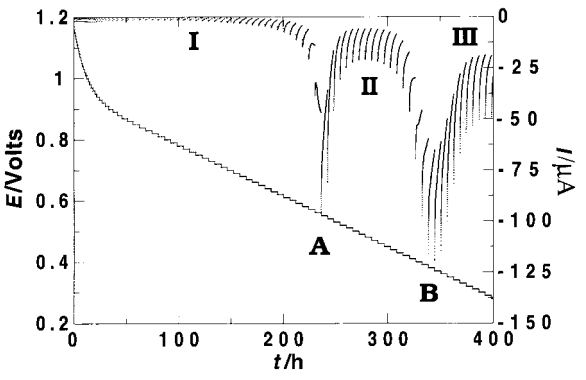

Fig. 2 Chronoamperogram obtained by discharging a cell Zn||WO_3 at a scan rate of −10 mV, 6 h

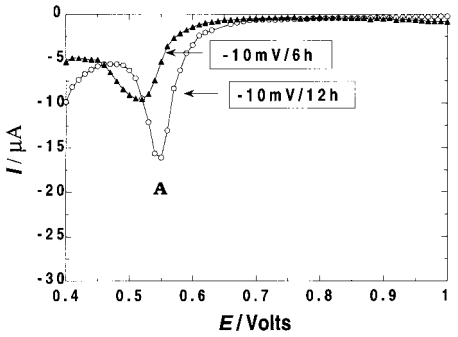

Fig. 3 A-peaks regions obtained for two different potentiostatic runs at different scan rates

On the basis of the experiment above described, we can conclude that zinc insertion in m-WO_3 proceeds through successive steps that involve the existence of single- and two-phase regions. The single phase domains correspond to the abrupt drops of the potential in the *E*-*x* plot (regions labelled as I, II and III) and with regions of minimum current in the *I*–*t* plot. On the other hand, plateaus in the voltage–composition plot and maxima of current in the *I*–*t* plot, where the behaviour of current with time does not follow a $t^{-1/2}$ law, correspond to two-phase domains. In both cases, the system shows a very slow reaction undoubtedly due to the double positive charge of zinc ions.

(*b*) Structural characterisation

In order to characterise the detected phases Zn_xWO_3 ($x=$ 0–0.01, 0.05–0.09 and 0.2–0.3) we have carried out a structural study. We have synthesised by electrochemical methods and characterised by X-ray diffraction several samples with composition Zn_xWO_3, where x corresponds to compositions belonging to different regions of the *E*–*x* diagram (I, II, III, A and B). Following the procedure described in the experimental section, several cells with configuration Zn|$Zn(CF_3SO_3)_2$ in PC–DMSO (1:4)|WO_3 were discharged at predetermined values of x.

The starting structure (WO_3 structure) is built up of apex-linked WO_6 octahedra forming an infinite tridimensional network of interconnecting tunnels typical of the ReO_3-type structure. At room temperature WO_3 is not cubic as is the ideal ReO_3, but monoclinic. However, as insertion proceeds, distortions from the ReO_3 cubic ideal symmetry tend to disappear.[2]

Fig. 4 shows the X-ray diffraction patterns of samples Zn_xWO_3 where $x=0.005$, 0.02, 0.06, 0.1 and 0.3. At low values of zinc concentration, $x<0.01$ [see *e.g.* $x=0.005$, Fig. 4(a)], the monoclinic WO_3 matrix is maintained although a certain loss of crystallinity is observed. Note that this sample corresponds to a region where a continuous variation of the potential with composition is detected (single phase assigned to region I in Fig. 1 and 2). As insertion proceeds a second abrupt change of potential is detected for a slight variation in composition (region II in Fig. 1 and 2). In this case a study by X-ray diffraction showed that, for samples with composition within this region [see *e.g.* $x=0.06$, Fig. 4(c)], a new phase, with variable composition and tetragonal symmetry, is formed. Between these solid solution regions the system, as proposed from the electrochemical results, should consist of a two-phase domain (region A in Fig. 1 and 2); indeed, we can see in Fig. 4(b) that the sample corresponding to this region, $x=$ 0.02, is mainly formed by a mixture of monoclinic and tetragonal phases.

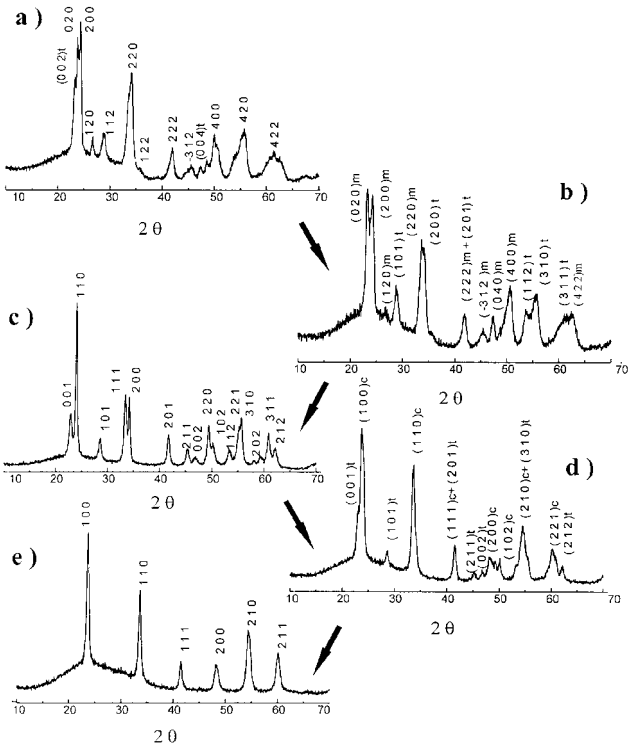

Fig. 4 X-ray diffraction patterns for some tungsten bronzes synthesised by zinc electrochemical intercalation: (a) $x=0.005$, (b) $x=0.02$, (c) $x=0.06$, (d) $x=0.1$ and (e) $x=0.3$ (c = cubic, t = tetragonal and m = monoclinic)

A similar situation is detected when zinc insertion proceeds at high ion concentration. Thus, for samples with compositions belonging to region III [see *e.g.*, $x=0.3$, Fig. 4(e)] the X-ray diffraction diagram shows the existence of a new phase of variable composition and cubic symmetry. On the other hand and in agreement with this reasoning, for region B a two-phase domain of tetragonal and cubic symmetry phases is observed [Fig. 4(d)].

From the electrochemical study of zinc insertion and the characterisation of the samples we can construct a phase diagram of the Zn-WO_3 system as shown in Fig. 5. Table 1 shows the phases formed in this system, their composition ranges and cell parameters which were calculated by a least square refinement program. All line positions were determined manually. Owing to the difficulty in obtaining high quality diffraction patterns, cell parameters are only approximate.

Note the good agreement between the different features detected in electrochemical plot E–x (and I–t diagram) and the phases detected by X-ray diffraction. This is a clear example of the usefulness of electrochemical techniques, in particular of

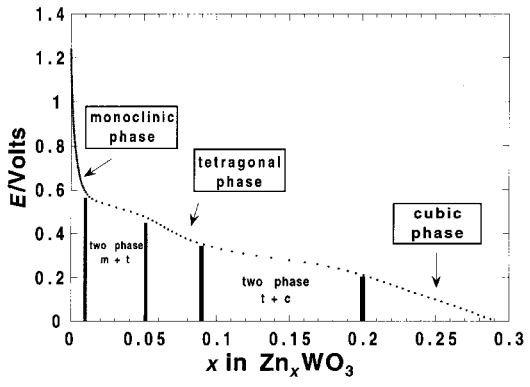

Fig. 5 A Zn–WO_3 'phase diagram' built from the combination of both electrochemical and structural data

Table 1 Phases of the system Zn–WO_3 and their cell parameters

range of existence	phase	cell parameters/Å
—	m-WO_3	$a=7.31(6)$, $b=7.53(4)$, $c=7.6(3)$, $\beta=90.(6)^\circ$
$0\leqslant x\leqslant 0.01$	monoclinic	$a=7.32(2)$, $b=7.52(7)$, $c=7.7(0)$, $\beta=90.(8)^\circ$ [a]
$0.01<x<0.05$	monoclinic + tetragonal	—
$0.05\leqslant x\leqslant 0.09$	tetragonal	$a=5.22(6)$, $c=3.87(9)$ [b]
$0.09<x<0.2$	tetragonal + cubic	—
$0.2\leqslant x\leqslant 0.3$	cubic	$a=3.76(9)$ [c]

[a]For a sample with composition $x=0.005$. [b]For a sample with composition $x=0.06$. [c]For a sample with composition $x=0.3$.

so-called electrochemical spectroscopy, to satisfactory characterise an insertion system.

(*c*) Other properties

The electrical properties of Zn_xWO_3 samples reflect the classical behaviour of tungsten bronzes in relation with the amount of ions inserted. Thus, when zinc is inserted in WO_3 (an insulator) its electrical conductivity increases by up to four orders of magnitude (for $Zn_{0.3}WO_3$). In the same way the colours of zinc tungsten bronzes show a dramatic change. Thus, as reaction proceeds the insertion compounds, originally green–yellow, develop different colours: initially sky blue, later deep blue and, finally blue violet for $Zn_{0.3}WO_3$. This latter colour is related to 0.6 electron/formula transfer between guest and host. The same colour is reported for $Na_{0.6}WO_3$[9] where the electron transfer is to the same extent.

Finally it should be mentioned that samples Zn_xWO_3 are unstable to air. After exposing them to the atmosphere they lose their colour reverting to the initial colour of the parent compound, *i.e.* green–yellow m-WO_3.

Conclusions

Zinc insertion in m-WO_3 has been studied and the existence of three single phases Zn_xWO_3 where $x=0$–0.01, 0.05–0.09 and 0.2–0.3 has been found. The transformation of the first to the second, and the second to the third, proceeds in both cases through a two-phase region. Different compositions in the whole range Zn_xWO_3 have been studied by X-ray diffraction, and the corresponding results perfectly correlate with the electrochemical characterisation. The first phase is monoclinic, the second tetragonal and the third cubic. For the whole range of composition, the system reacts slowly and this is likely to be due to the double positive charge of zinc ions.

A.M.C. wants to thank UANL (Mexico) for making possible the stay at Universidad Complutense. The authors would like to thank CICYT (Spain) through grant MAT95-0809 for financial support. F.G.-A. also thanks Universidad San Pablo-CEU for supporting the project 8/97.

References

1 P. Hagenmuller, in *Comprehensive Inorganic Chemistry*, Pergamon, Oxford, 1973, vol. 4, p. 572.
2 B. W. Brown and E. Banks, *J. Am. Chem. Soc.*, 1954, **76**, 963.
3 Y. Chabre, *J. Electrochem. Soc.*, 1991, **138**, 329.
4 J. M. Tarascon, *J. Electrochem. Soc.*, 1985, **132**, 2089.
5 R. E. Duber, S. Patat and P. G. Dickens, *Solid State Ionics*, 1995, **80**, 231.
6 W. Weppner, in *The CRC Handbook of Solid State Electrochemistry*, ed. P. J. Gellings and H. J. M. Bouwmeester, CRC Press, New York, 1997, p. 285.
7 J. A. Perri, E. Banks and B.Post, *J. Appl. Phys.*, 1957, **28**, 1272.
8 Y. Chabre and J. Pannetier, *Prog. Solid State Chem.*, 1995, **23**, 1.
9 M. S. Whittingham, in *Intercalation Chemistry*, ed. M. S. Whittingham and A. J. Jacobson, Academic Press, New York, 1982, p. 8.

Paper 8/01461B; *Received* 20*th February*, 1998